1999

Raman characterization of alkanethiols and the application of alkanethiols to electroreflectance spectroscopy

Albert Avila
Iowa State University

INFORMATION TO USERS

This manuscript has been reproduced from the microfilm master. UMI films the text directly from the original or copy submitted. Thus, some thesis and dissertation copies are in typewriter face, while others may be from any type of computer printer.

The quality of this reproduction is dependent upon the quality of the copy submitted. Broken or indistinct print, colored or poor quality illustrations and photographs, print bleedthrough, substandard margins, and improper alignment can adversely affect reproduction.

In the unlikely event that the author did not send UMI a complete manuscript and there are missing pages, these will be noted. Also, if unauthorized copyright material had to be removed, a note will indicate the deletion.

Oversize materials (e.g., maps, drawings, charts) are reproduced by sectioning the original, beginning at the upper left-hand corner and continuing from left to right in equal sections with small overlaps. Each original is also photographed in one exposure and is included in reduced form at the back of the book.

Photographs included in the original manuscript have been reproduced xerographically in this copy. Higher quality 6" x 9" black and white photographic prints are available for any photographs or illustrations appearing in this copy for an additional charge. Contact UMI directly to order.

UMI®

Bell & Howell Information and Learning
300 North Zeeb Road, Ann Arbor, MI 48106-1346 USA
800-521-0600

Raman characterization of alkanethiols and the application of alkanethiols to electroreflectance spectroscopy

by

Albert Avila

A dissertation submitted to the graduate faculty

in partial fulfillment of the requirements for the degree of

DOCTOR OF PHILOSOPHY

Major: Analytical Chemistry

Major Professor: Dennis Johnson

Iowa State University

Ames, Iowa

1999

Graduate College
Iowa State University

This is to certify that the Doctoral dissertation of

Albert Avila

has met the dissertation requirements of Iowa State University

Signature was redacted for privacy.
Major Professor

Signature was redacted for privacy.
For the Major Program

Signature was redacted for privacy.
For the Graduate College

To my wife Jackie, my family and friends
whose love and encouragement helped
make this dissertation possible.

TABLE OF CONTENTS

LIST OF ABBREVIATIONS

CV	Cyclic voltammetry
cyt. *c*	Cytochrome *c*
EM	Electromagnetic
ER	Electroreflectance
ET	Electron-transfer
FWHM	Full width half maximum
GC	Gas chromatography
GC/MS	Gas chromatography/mass spectroscopy
HPLC	High pressure liquid chromatography
Im	Imaginary (component)
NMR	Nuclear magnetic resonance
PMT	Photomultiplier tube
Re	Real (component)
SAM(s)	Self-assembled monolayer(s)
SCE	Saturated calomel electrode
SEERS	Surface-enhanced electronic Raman scattering
SERS	Surface-enhanced Raman scattering
TLC	Thin layer chromatography
UV-Vis	Ultraviolet-visible

CHAPTER 1. GENERAL INTRODUCTION

The characterization and applications of self-assembled monolayers (SAMs), especially alkanethiol SAMs on metal surfaces, are increasingly yielding useful information in the field of surface chemistry. Despite previous investigations of the structure of alkanethiol SAMs, there are several issues which need to be resolved. Understanding these issues is very important in order to fully characterize these monolayers and determine their proper structures. This information is also critical to the application of these alkanethiol SAMs in the fields of surface chemistry. One critical area in which these monolayers can be applied is as a pathway for electron-transfer between electrodes and redox proteins.

The research objectives of this dissertation can be divided into two main sections. The first section involves the characterization of various alkanethiol SAMs on coinage metal surfaces. Novel Raman bands have been observed and possible sources of the band investigated. The second section involves the application of alkanethiol SAMs on gold electrodes as model systems to study biological electron-transfer reactions. The alkanethiol SAMs serve as biomimetic membranes to immobilize proteins for study.

Dissertation Organization

Chapter 1 is a general background of the two most important areas and techniques related to this dissertation research. The first section examines surface-enhanced Raman scattering (SERS), which is used extensively in this dissertation. A brief review of SERS theory and analytical applications of SERS described. The second section examines the

technique of electroreflectance (ER) spectroscopy. A review of ER spectroscopy and its applications to electron-transfer rate measurements are provided.

Chapter 2 is a characterization of various alkanethiol SAMs on gold electrodes and colloids and silver electrodes. A series of previously unknown Raman bands are observed within a broad excitation range under a variety of conditions. This research centers on efforts to determine the source of the new bands using SERS and a variety of other techniques. This chapter is a paper to be submitted to the *Journal of the American Chemical Society*. Chapter 3 is an extension of the research involving the SAMs of alkanethiols on metal surfaces. The efforts in this chapter focus on a possible source of the previously unknown Raman bands due to image states on the metal surface. This work has been submitted to the *Journal of Physical Chemistry*.

Chapter 4 is a paper submitted to *Biochemistry*. This work involves the application of alkanethiol monolayers as spacer molecules (membrane models) between gold electrodes and immobilized cytochrome *c*. The effects of electrolyte solution pH and ionic strength on electron-transfer reactions are determined using potential modulated ER spectroscopy. Chapter 5 is a paper submitted to the *Journal of Biological Inorganic Chemistry*. Alkanethiol monolayers are again employed as spacer molecules (membrane models) between gold electrodes and immobilized cytochrome *c*. Electrolyte solution viscosity is varied and the effects on electron-transfer reactions are determined utilizing potential modulated ER spectroscopy. SERS is applied to confirm the native state of the immobilized cyt. *c* as the viscosity is changed. Chapter 6 is a brief section on general conclusions of research achievements and possible directions for future work.

Surface-Enhanced Raman Spectroscopy

A strong increase in Raman scattering intensity has been observed for molecules and ions that are close to or adsorbed on certain metallic surfaces. This phenomenon, known as surface-enhanced Raman scattering (SERS), can lead to intensity enhancement factors of 10^5 to 10^6 relative to the Raman scattering in the absence of the metal surface.[1-3] SERS is employed as an important tool in the present dissertation work to characterize alkanethiol monolayers on gold and silver surfaces.

The SERS effect was discovered by electrochemists in the early 1970s in efforts to study adsorption processes at metal electrodes in aqueous solutions.[4-6] As study of the pyridine-Ag system continued, researchers noted the large enhancement in Raman scattering at the electrode surface. Since the early 1980s, many efforts have been made to understand the SERS enhancement mechanisms.[7-9] Other studies have applied the SERS effect as a spectroscopic tool in areas such as chemistry, biochemistry and material science.[2,10-11]

Theoretical Considerations

The classical treatment of light scattering examines particles which are much smaller (typically $\leq \lambda_L/15$) than the wavelength of the incident radiation.[12] In such cases, a particle can be polarized by the electric field **E** of the incident radiation, inducing a dipole moment μ in the particle. The induced dipole moment is expressed by

$$\mu = \alpha \cdot \mathbf{E} \qquad (1)$$

where α is the polarizability of the particle. The polarizability, a tensor quantity, can be thought of as a deformation of the particle's electron cloud by the incident electric field **E**. In

cases where the particle is a molecule whose atoms can vibrate at a frequency ω_k, a time dependence t is introduced into the polarizability α, which can be shown as

$$\alpha = \alpha_o + \cos(\omega_k t) \qquad (2)$$

where α_o is the polarizability of the molecule at its equilibrium geometry.[2] A time dependence is also present in **E** which varies with the frequency of the light ω_L.

$$\mathbf{E} = \mathbf{E}_o \cos(\omega_L t) \qquad (3)$$

Equations (2) and (3) are substituted into equation (1), followed by expansion of the equation to include the time-dependent terms. Simplification of the equation yields the expression

$$\mu(\omega_L) = \alpha_o \mathbf{E}_o \cos(\omega_L t) + (\tfrac{1}{2})\alpha_o \mathbf{E}_o \cos(\omega_L - \omega_k)t + (\tfrac{1}{2})\alpha_o \mathbf{E}_o \cos(\omega_L + \omega_k)t \qquad (4)$$

The first term on the right side of equation (4) describes Rayleigh scattering. This "elastically" scattered light emerges from the sample at the same frequency as the incident light. The second and third terms are Raman scattering in which this "inelastically" scattered light is shifted in frequency relative to the incident light. The frequency shifts are determined by vibrational frequencies of the molecule and measurement of these shifts yields information on the scattering molecules. The second term is Stokes Raman scattering where the scattered light is red-shifted relative to the incident light while the anti-Stokes Raman scattering of the third term is blue-shifted. Statistical thermodynamic treatments of Raman scattering (the Boltzmann distribution function) predict that the Stokes bands have a larger intensity than the anti-Stokes bands, therefore only the Stokes spectra are usually collected in normal Raman.

If the molecules of interest are adsorbed on or near the surface of certain metals (notably Ag, Au and Cu), the intensity of the Raman scattering is greatly enhanced. These metal surfaces are generally referred to as "SERS-active" and usually visible light is used as

incident radiation. The theories proposed to explain SERS are divided into two broad categories, as expected from equation (1). These two broad categories are known as electromagnetic (EM) enhancement mechanisms and chemical enhancement mechanisms.

The EM enhancement mechanisms propose a large increase in the electromagnetic field **E** exerted on the molecules on or near the metal surface. The EM field exerted on these molecules is modified in several ways. First, the incident EM field is enhanced through the polarization of the metal surface that allows the metal to act as a mirror, allowing the adsorbed molecules to be exposed to larger EM fields.[2] Second, the incident EM field polarizes adsorbed molecules. The vibrations of these polarized molecules induce plasmon oscillations on the metal surface, causing the surface to radiate at vibrational frequencies of the adsorbed molecules.[13] Third, the lifetimes of molecular excited states can be changed by energy transfer between the adsorbed molecule and the metal surface. It is thought that structures with very small radii of curvature produce these three effects most efficiently.[9,14]

EM enhancement theories have generally been useful in accounting for several experimental observations of SERS.[2,3] Surface roughness is necessary for the SERS substrate and these roughness features (ex. adatoms, clusters, particles, dislocations, islands) provide sites where the EM field is greatly magnified. Metal specificity and excitation wavelength dependence can generally be accounted for by EM theories since only specific metals with the "right" optical properties enhance the SERS signal. Excitation profiles of a given vibrational mode (Raman intensity vs. $h\omega$) of SERS active compounds show band intensity increases as the excitation frequency decreases, counter to the ω^4 dependence of normal Raman. A distance dependence effect in SERS can also be explained with the EM theories. A SERS

dependence of $(\alpha/r)^{12}$, where α is the radius of curvature for the surface roughness features and r is the distance of the adsorbed molecule to the metal surface, has been observed therefore molecules of interest do not have to be in direct contact with the metal surface to get SERS.

The chemical enhancement mechanisms propose large increases in adsorbate polarizability due to the interaction of the adsorbate with the metal surface to form a surface complex.[2,3] Some chemical enhancement theories suggest that SERS arises from the interaction of adsorbates with metal adatoms or clusters on the electrode surface. Other enhancement theories maintain that the SERS effect originates from metal/adsorbate charge-transfer or electron-hole pair creation. Chemical enhancement mechanisms tend to exhibit adsorbate specificity due to the interactions of the molecules of interest and the metal surface. For the most part, the chemical enhancement mechanisms are more difficult to test experimentally.

Chemical enhancement theories have generally been successful in explaining several SERS observations. It has been noted that a degree of adsorbate specificity exists since many compounds and ions do not yield high quality SERS spectra yet nitrogen and sulfur containing species exhibit very good SERS. A "relaxation" of selection rules in SERS is possible due to the presence of the metal surface; bands not seen in the bulk may be observed by SERS. Band frequencies and relative band intensities obtained by SERS often differ from those from bulk samples.[15] Finally, a Raman band potential dependence has been observed for certain adsorbed molecules on SERS active electrodes. Raman band position shifts and changes in their relative intensities can vary with applied SERS electrode potential.

Alone, neither EM nor chemical enhancement mechanisms can fully account for all experimental observations involved with SERS. When taken together, the EM and chemical enhancement mechanisms offer methods to predict the overall behavior of SERS systems. The total SERS enhancement is likely to be a product of both enhancement mechanisms.

Analytical Applications of SERS

The application of SERS to analytical problems has been demonstrated as an effective method for both qualitative and quantitative analysis.[16] Recent applications of SERS based detection systems have been centered in the areas of gas chromatography, thin layer chromatography and flow injection analysis. Several problems have been encountered with the application of SERS to detection systems which have been overcome by novel means. These problems include a) long term stability of the metal surface, b) fouling of the electrode surface by strongly adsorbing species or weak adsorption by desired compounds, 3) reproducibility of SERS intensities at different electrode sites and 4) calibration curves that are linear over a small dynamic range.

SERS detection for GC was demonstrated by Roth by trapping pyridine effluent in Ag colloid solutions and on colloid modified TLC plates.[17] Another GC-SERS detection approach was based on a 1-propanethiol modified Ag foil, as demonstrated by Carron.[18] The alkanethiol modified Ag electrode promoted adsorption of organic species on the electrode without fouling and prevented the Ag electrode from oxidation. The application of SERS to TLC has recently be reviewed by Somsen and coworkers.[19] Newer applications of SERS to TLC include work by Matejka and coworkers to detect aromatic hydrocarbons using Ag activated TLC plates.[20] Caudin and coworkers employed Ag colloid precoated TLC plates to

detect sub-femtogram amounts of crocetin with FT-Raman techniques.[21] SERS applications to flow injection analysis and liquid chromatography have been achieved by several groups. Cabalin and coworkers have utilized mixing fresh Ag colloid with the column eluent to detect various drugs in biological samples.[22,23] Another approach involved a computer controlled potential waveform to adsorb/desorb analytes at an Ag foil electrode.[24] Potential modulation of the Ag foil alternately cleaned the electrode and provided a fresh SERS electrode. An alternate method demonstrated by Rubim and coworkers involved the introduction of Ag^+ ion into the flow system, followed by electrodeposition of Ag onto a glassy carbon electrode.[25] Anodic stripping is used to clean the carbon electrode between analytes and maintain a stable SERS active surface.

Thus it appears that SERS is a practical technique for routine analysis. SERS provides the high sensitivity, molecular specificity and low detection limits necessary for analytical applications.

Electroreflectance Spectroscopy

Electroreflectance spectroscopy is one of the surface sensitive techniques that combine the areas of spectroscopy and electrochemistry. In essence, electroreflectance spectroscopy determines the change in reflectivity R of a solid/electrolyte interface resulting from a change in electrode potential E ($\delta R/\delta E$).[26] This change in reflectivity may or may not be accompanied by a faradaic reaction. The benefits ER spectroscopy has to offer for electrode surface study include the determination of information on a molecular level, the nondestructive nature of the experiments and its application *in situ*.[27] The relatively simple ER instrumental setup and the

use of any light-reflective electrode material contribute to its usefulness. Unless a highly colored electrolyte solution is used, it is generally not necessary to use thin-layer cells, as is necessary for IR reflection measurements. Another advantage of the ER technique is the ability to measure faradaic processes at the electrode as an optical response. The double layer charging effects on the ET reaction measurement are eliminated when ER is utilized, as compared to other electrochemical techniques.

Theoretical Considerations

In this treatment of ER theory for electron-transfer (ET) rate determination, it is considered that UV-Vis reflectance measurements are conducted at an electrode/solution interface where the electrode is covered with a thin film (or monolayer) of an electroactive species.[28] The solution in which the electrode is immersed is free of electroactive species. It is also noted that if the electroactive species has a strong absorption band which can be altered by a change in electrode potential, then a spectral change of the film can be obtained by the application of an ac signal to the electrode.[27] The UV-Vis reflectance spectra can be determined by several modulation techniques, however electrode potential modulation is surface sensitive and relatively easy to employ. The chemical reaction of the adsorbed species can be reduction/oxidation (redox) or adsorption/desorption.

The equivalent circuit of the molecular reaction on the electrode surface is shown in Figure I where R_s is the solution resistance, C_d the double-layer capacitance, R_{ct} the charge transfer resistance and C_a the capacitance induced by the adsorbed redox species. E_T is the total ac voltage across the equivalent circuit while E_F is the ac voltage due to the faradaic

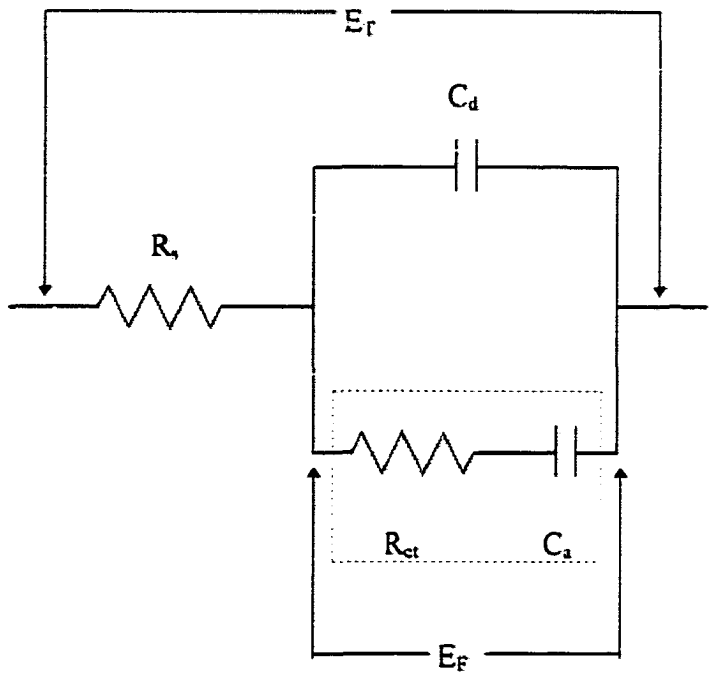

Figure 1. Equivalent circuit of the molecular reaction on the electrode surface. The dotted box shows the faradaic portion of the circuit. See text for notations.

component of the circuit. A total potential E can be applied to the ER working electrode as shown in equation (5)

$$E = E_{dc} + E_{ac} = E_{dc} + \Delta E_{ac} \exp(i\omega t) \quad (5)$$

where E_{dc} is a dc potential, E_{ac} an ac potential, ΔE_{ac} the ac amplitude, ω the frequency of ac modulation and t is time. If E_{dc} is set to the $E^{o'}$ of a redox reaction and ΔE_{ac} is much smaller than RT/n_aF, then by linear approximation R_{ct} and C_a can be expressed *for the equivalent circuit* by the following equations.[29-31]

$$R_{ct} = 2RT / nn_aF^2k_s\Gamma_t \quad (6)$$

$$C_a = nn_aF^2\Gamma_t / 4RT \quad (7)$$

In equations (6) and (7) R is the gas constant, T the absolute temperature, n the number of electrons involved in the redox reaction, n_a the apparent number of electrons[28], F the Faraday constant and Γ_t the total surface concentration of the redox species. Substitution of equation (7) into equation (6) and solving for the electron-transfer reaction rate constant k_s yields

$$k_s = (2R_{ct}C_a)^{-1} \tag{8}$$

Equation (8) is applicable only to the *equivalent circuit*. ER does not directly determine R_{ct} and C_a, but the change in reflectance. The reflectomittance Y_A of the equivalent circuit can be thought of as the change in reflectivity as the electrode potential is modulated.[28] With lock-in amplifier detection, the ac reflectance and potential signals are determined over the entire circuit and can be written as

$$R_T = Y_A E_T \tag{9}$$

Application of circuit theory to equation (9) in terms of R_{ct}, R_s, C_a, and C_d and solving for Y_A yields the real and imaginary parts of Y_A, which are the values actually determined by lock-in detection.

$$\mathrm{Re}\,(Y_A) = -KC_a(1-\omega^2R_sR_{ct}C_aC_d) / \xi \tag{10}$$

$$\mathrm{Im}\,(Y_A) = KC_a\omega\,(R_{ct}C_a + R_sC_a + R_sC_d) / \xi \tag{11}$$

where K is a difference absorption coefficient between the reduced and oxidized forms and

$$\xi = (1-\omega^2R_sR_{ct}C_aC_d)^2 + \omega^2(R_{ct}C_a + R_sC_a + R_sC_d)^2 \tag{12}$$

The relation $\cot\phi = \mathrm{Re}\,(Y_A) / \mathrm{Im}\,(Y_A)$ in addition to equations (10) and (11) produce

$$-\omega\cot\phi = (1-\omega^2R_sR_{ct}C_aC_d) / (R_{ct}C_a + R_sC_a + R_sC_d) \tag{13}$$

where ϕ is the phase angle between R_T and E_T. The solution resistance, R_s, and double layer charging, C_d, in equation (13) are measurable quantities of the ER cell. A plot of $\omega\cot\phi$ vs.

ω^2 is used to determine slope and y-intercept data from different applied ac frequencies. The y-intercept is equal to $1 / (R_{ct}C_a + R_sC_a + R_sC_d)$ while the slope is equal to $(R_sR_{ct}C_aC_d) / (R_{ct}C_a + R_sC_a + R_sC_d)$. Determination of the y-intercept, followed by the application of R_s and C_d to the slope term enable the values of R_{ct} and C_a to be calculated. The apparent ET reaction rate constant can then be determined from R_{ct} and C_a.

Previous Studies

ER spectroscopy has been applied to the investigation of electrode reactions for several organic species. Sagara and coworkers employed ER spectroscopy to determine monolayer characteristics and ET rates of methylene blue adsorbed on pyrolytic graphite electrodes.[32-34] These papers described ER theory and established some acquisition parameters as applied to monolayer study. Various orientation effects were also noted while using polarized light. The investigation of physical and chemical changes in monolayers of heptylviolgen on Ag electrodes was performed by Wang and coworkers.[35] These workers found that different aggregation states of cation radicals were formed on the Ag surfaces over time which led to different ET rates. Work by Feng and coworkers centered on determining ET rates of cyt. *c* through alkanethiol monolayers.[36-38] These studies investigated the ET rate dependence on alkanethiol chain length and noted the effects of varying instrumental parameters and experimental conditions. ER spectroscopy has also been employed to investigate ET through mixed monolayers of alkanethiols.[39]

It appears that ER spectroscopy is an excellent method to determine ET rates on electrode surfaces. Its ease of use, nondestructive nature and general applicability to surface studies contribute to its increasing application as an analytical tool.

References

(1) Otto, A. *J. Phys.: Condens. Matter* **1992**, *4*, 1143.

(2) Brandt, E. S.; Cotton, T. M. In *Investigations of Surfaces and Interfaces-Part B*, 2nd ed.; Rossiter, B. W. and Baetzold, R. C., Eds.; Physical Methods of Chemistry Series; Wiley: New York, 1993, 633.

(3) Birke, R. L.; Lombardi, J. R. In *Spectroelectrochemistry: Theory and Practice*, 1st ed.; Gale, R. J., Eds.; Plenum Press: New York, 1988, 263.

(4) Fleishcmann, M.; Hendra. P.J.; McQuillan, A. J. *Chem. Phys. Lett.* **1974**, *26*, 163.

(5) Albrecht, M. G.; Creighton, J. A. *J. Am. Chem. Soc.* **1977**, *99*, 5215.

(6) Jeanmaire, D. L.; Van Duyne, R. P. *J. Electroanal. Chem.* **1977**, *84*, 1.

(7) Moskovits, M. *Rev. Mod. Phys.* **1985**, *57*, 783.

(8) Chang, R. K.; Furtak, T. E. *Surface Enhanced Raman Scattering*; Chang, R. K.; Furtak, T. E., Eds.; Plenum Press: New York, 1982.

(9) Otto, A.; Mrozek, I.; Grabhorn. H.; Akemann, W. J. *Phys.: Condens. Matter* **1992**, *4*, 1143.

(10) Garrell, R. L. *Anal. Chem.* **1989**, *61*, 410A.

(11) Rupérez, A.; Laserna, J. J. In *Modern Techniques in Raman Spectroscopy*, Laserna, J. J., Ed.; Wiley: New York, 1996, 227.

(12) Van de Hulst, H. C. *Light Scattering By Small Particles*, Dover: New York, 1981.

(13) Kerker, M. *Acc. Chem. Res.* **1984**, *17*, 271.

(14) Zeman, E. J.; Schatz, G. C. *J. Phys. Chem.* **1987**, *91*, 634.

(15) Cotton, T. M.; Kim, J. H.; Chumanov, G. D. *J. Raman Spectrosc.* **1991**, *22*, 279.

(16) Garrell, R. L. *Anal. Chem.* **1989**, *61*, 401A.

(17) Roth, E.; Kiefer, W. *Appl. Spectrosc.* **1994**, *48*, 1193.

(18) Carron, K. T.; Kennedy, B. J. *Anal. Chem.* **1995**, *67*, 3353.

(19) Somsen, G. W.; Morden, W.; Wilson, I. D. *J. Chromatogr. A* **1995**, *703*, 613.

(20) Matejka, P.; Stavek, J.; Volka, K.; Schrader, B. *Appl. Spectrosc.* **1996**, *50*, 409.

(21) Caudin, J. P.; Beljebbar, A.; Sockalingum, G. D.; Angiboust, J. F.; Manfait, M. *Spectrochim. Acta* **1995**, *51*, 1977.

(22) Cabalin, L. M.; Ruperez, A.; Laserna, J. J. *Talanta* **1993**, *40*, 1741.

(23) Cabalin, L. M.; Ruperez, A.; Laserna, J. J. *Anal. Chim. Acta* **1996**, *318*, 203.

(24) Pothier, N. J.; Force, R. K. *Appl. Spectrosc.* **1994**, *48*, 421.

(25) Gouveia, V. J.; Gutz, I. G.; Rubin, J. C. *J. Electroanal. Chem.* **1994**, *371*, 37.

(26) Kolb, D. M. In *Spectroelectrochemistry: Theory and Practice*, 1st ed.; Gale, R. J., Eds.; Plenum Press: New York, 1988, 87.

(27) Sagara, T. *Recent Res. Devel. in Physical Chem.* **1998**, *2*, 159.

(28) Feng, Z. Q.; Sagara, T.; Niki, K. *Anal. Chem.* **1995**, *67*, 3564.

(29) Sagara, T.; Niwa, K.; Sone, A.; Hinnen, C.; Niki, K. *Langmuir* **1990**, *6*, 254.

(30) Lelieve, D.; Plichon, V.; Laviron, E. *J. Electroanal. Chem.* **1980**, *112*, 137.

(31) Laviron, E. *J. Electroanal. Chem.* **1979**, *97*, 135.

(32) Sagara, T.; Igarashi, S.; Sato, H.; Niki, K. *Langmuir*, **1991**, *7*, 1005.

(33) Sagara, T.; Iizuka, J.; Niki, K. *Langmuir*, **1992**, *8*, 1018.

(34) Sagara, T.; Niki, K. *Langmuir*, **1993**, *9*, 831.

(35) Wang, H. X.; Sagara, T.; Sato, H.; Niki, K. *J. Electroanal. Chem.* **1992**, *331*, 925.

(36) Feng, Z. Q.; Imabayashi, S.; Kakiuchi, T.; Niki, K. *J. Electroanal. Chem.* **1995**, *349*, 149.

(37) Feng, Z. Q.; Imabayashi, S.; Kakiuchi, T.; Niki, K. *J. Electroanal. Chem.* **1996**, *408*, 15.

(38) Feng, Z. Q.; Imabayashi, S.; Kakiuchi, T.; Niki, K. *J. Chem. Soc., Faraday Trans.* **1997**, *93*(7), 1367.

(39) Arnold, S.; Feng, Z. Q.; Kakiuchi, T., Knoll, W.; Niki, K. *J. Electroanal. Chem.* **1997**, *438*, 91.

CHAPTER 2. INVESTIGATION OF THE SERS RESPONSE OF ALKANETHIOLS ON METAL ELECTRODES

A paper to be submitted to the *Journal of the American Chemical Society*

Albert Avila, Brian W. Gregory and Therese M. Cotton

ABSTRACT

A series of novel Raman bands has been observed in the surface-enhanced Raman scattering (SERS) spectra of self assembled monolayers (SAMs) of alkanethiols on Au and Ag surfaces. The novel Raman bands display a resonance effect, observed with excitation in the 630 to 710 nm range. The bands exhibit a chain length dependence at room temperature, occurring in SAMs with $n \geq 9$ methylene groups. At liquid nitrogen temperatures, SAMs with $n \geq 6$ display the bands, indicating a dependence on monolayer structure. Alkanethiol isotopic labeling studies involving substitutions of ^{2}H, ^{13}C and ^{34}S reveal that the novel bands are not likely of a vibrational origin. In addition, SAMs of $(CH_3\text{-}(CH_2)_9\text{-}Se)_2$ on Au yield identical spectra (within $\pm$ 1 cm^{-1}) as the alkanethiol SAMs. Electrode potential studies of SERS have shown that charge transfer effects are not the source of the bands. Impurities on the SERS electrode surfaces do not appear to be source of the novel bands.

INTRODUCTION

The self-assembly of molecules to form monolayers, especially alkanethiols, on Au and Ag metal surfaces has been extensively studied in the past several years.[1-4] The relative ease of alkanethiol monolayer preparation, their well-ordered structure and their general ruggedness have all contributed to their study. The affinity of the thiol headgroup for a

variety of metal surfaces offers a wide range of materials to study monolayers. These benefits have been exploited in a variety of research areas, including electron-transfer[5], membrane modeling[6] and corrosion[7]. Variation of the alkanethiol monolayer properties can be achieved by the careful selection of terminal groups, carbon chain lengths and chain modification.

Analytical techniques such as electrochemistry[4], IR spectroscopy[8], XPS[9], electron diffraction[10] and ellipsometry[11] have indicated that highly ordered alkanethiol monolayers are formed on Au surfaces. The substrates used in the majority of this work have been Au(111) surfaces. Early diffraction and scanning probe microscopy studies of methyl-terminated alkanethiols on Au(111) indicated a simple $(\sqrt{3} \times \sqrt{3})R30°$ monolayer structure.[12] Later studies have demonstrated the existence of a c(4 x 2) superlattice of alkanethiol molecules on the Au surface.[13] Although these data yield much information on alkanethiol monolayer structure, they do not reveal much about the bonding of the sulfur headgroup and the Au surface.

IR spectroscopy has been the technique most commonly employed to determine vibrational information from the alkanethiol monolayers.[8] Spectral information of the alkanethiols has for the most part been determined from the ν(C-H) region since the many C-H bonds along the carbon chain yield a relatively strong IR signal. Various modes have been identified in this region which indicate relatively dense carbon chain packing. In contrast, direct vibrational information in the ν(C-S) region is lacking since these bands are relatively weak in the IR.[14] The use of Raman spectroscopy, especially surface-enhanced Raman scattering (SERS), is another technique which can determine additional vibrational information about these monolayers.

There have been several previous reports on the application of Raman spectroscopy to study thiol monolayers on Au and Ag surfaces.[1,15-19] A number of these reports have involved aromatic thiols.[15] The orientation of benzenethiol and other aromatic compounds on Au surfaces were deduced. Some reports have involved straight chain thiols on Au and Ag surfaces, mostly short chain alkanethiols.[17] The formation of 1-propanethiol and 1-butanethiol on roughened Au surfaces has shown some aspects of chain packing. A few studies have focused on longer carbon chain alkanethiols, most notably work by Bryant and Pemberton.[18,19] These workers have assigned the ν(C-H), ν(C-C) and ν(C-S) bands in the SERS spectra obtained on both Au and Ag surfaces. The authors also rationalize the surface selection rule arguments which explain the differences in SERS spectra observed between the two metals. Recently we have discovered several new bands in the SERS spectra for straight chain alkanethiols on both Au and Ag surfaces. These new bands are only observed in a limited excitation range and for longer chain lengths. This report describes the new SERS bands, the monolayers giving rise to the new bands, and the experimental results relating to their possible sources.

EXPERIMENTAL

Materials. All alkanethiol solutions were freshly prepared in HPLC grade methanol from Fisher Scientific or punctilious grade ethanol from Quantum Chemical Co. A number of alkanethiols, including 1-butanethiol (99%), 1-hexanethiol (95%), 1-octanethiol (97+%), 1-nonanethiol (95%), 1-decanethiol (96%), 1-dodecanethiol (98%), 1-hexadecanethiol (92%)

and 1-octadecanethiol (98%), were purchased from Aldrich Chemical and used as received. 1-Tetradecanethiol was purchased from Pfaltz & Bauer Chemical and used as received.

11-Mercapto-1-undecanol and 12-mercapto-1-dodecanol were prepared in our laboratory by a modification of literature procedures.[20] The starting compounds, 11-bromo-1-undecanol (98%) and 12-bromo-1-dodecanol (99%), were purchased from Aldrich Chemical and used as received. Thiourea (99+%) was purchased from Sigma Chemical Co. and used as received. Briefly, equal molar amounts of the ω-bromo-1-alcohol and thiourea were refluxed in 95% ethanol for three hours, followed by the addition of aqueous base and refluxed for an additional two hours. The solutions were cooled, neutralized with dilute H_2SO_4 and the ω-mercaptoalcohols were extracted from the aqueous solutions. The synthesized mercaptoalcohols were washed with HPLC grade methanol and 18 MΩ cm water to remove impurities and vacuum dried. GC/MS analysis demonstrated the desired mercaptoalcohols were synthesized with an estimated 98% purity.

The synthesis of didecyl diselenide was a modification of the alkanethiol procedure.[20] The starting compounds, 1-bromodecane and selenourea were purchased from Aldrich Chemical and used as received. Equal molar amounts of 1-bromodecane and selenourea were refluxed in 95% ethanol for approximately four (4) hours under a nitrogen atmosphere. Aqueous base was added and the solution refluxed for approximately three (3) additional hours. Despite the nitrogen atmosphere during the synthesis, the formation of diselenide instead of 1-decaneselenol occurred due to the traces of oxygen in the reaction vessel. The didecyl diselenide formed as a yellow oil and then separated from the aqueous reaction mixture. The aqueous fraction of the reaction mixture was acidified with dilute H_2SO_4, and

extracted with hexane to yield additional diselenide. The diselenide fractions were added together and placed on a Buchner Rota-vap to remove any remaining hexane and ethanol. GC/MS analysis demonstrated the desired diselenide was synthesized with an estimated 98% purity.

Solutions prepared for self-assembly typically contained total alkanethiol or dialkanediselenide concentrations of approximately 1 to 5 mM in methanol or ethanol. Both Ag and Au electrodes were exposed to the deposition solutions overnight (minimum of 10 hours) at room temperature unless otherwise noted. The electrodes were rinsed with fresh methanol or ethanol upon removal from the solutions.

The water used in these experiments was distilled and then deionized using a Millipore Milli-Q water system. Low temperature experiments were performed using 200 proof punctilious ethanol obtained from Quantum Chemical Company and used as received. The ethanol was mixed with liquid nitrogen to form a slurry with temperatures as low as -30°C.

Sodium citrate for colloid preparation was purchased from Fisher Scientific and used as received. Hydrogen tetrachloroaurate(III), sodium tetrachloroaurate(III) dihydrate, silver nitrate and 2,2'-thiodiethanol were purchased from Aldrich and used as received.

Electrode Preparation. The electrodes were prepared from either polycrystalline Au foil or polycrystalline Ag or Au rod electrodes press-fitted into Teflon shrouds. The Au foil electrodes were initially placed in warm concentrated nitric acid for approximately 30 minutes to remove surface impurities and then sonicated several times in 18 MΩ cm water. The Au foil electrodes were then flame annealed to achieve a smoother, more uniform surface. The Teflon shrouded electrodes were initially polished with successively finer gradations of

alumina paste until they had a mirror-like optical finish and were subsequently sonicated in 18 MΩ cm water. Afterwards, the Teflon shrouded Au electrodes were immersed in 9 M HNO_3 for approx. 3-5 s, followed by sonication in 18 MΩ cm water. The Ag electrodes were electrochemically roughened by oxidation-reduction cycles (ORC) in 0.1 M Na_2SO_4 solution followed by rinsing and storing in 18 MΩ cm water. The Au foil electrodes were roughened by 400-1000 ORCs consisting of potential steps between +1.3 and -0.3 V vs. a saturated calomel electrode (SCE) followed by a 2 s rest at -0.3 V. The Teflon shrouded Au rod electrodes were roughened by 40 ORCs consisting of potential ramps of 500 mV/s between +1.3 and -0.3 V vs. SCE. All Au electrodes were roughened in 0.1 KCl solution and then rinsed and stored in 18 MΩ cm water. Immediately before exposure to the alkanethiol solutions, the electrodes were dipped in HPLC grade methanol or ethanol to remove excess water. The electrodes were exposed to the alkanethiol solutions within 1 hour of preparation.

Colloid Preparation. Au colloid was prepared in 500 mL batches using a literature method.[21] Ag colloid was prepared using a citrate reduction proceedure.[22]

Raman Instrumentation and Experimental Conditions. The 514.5 nm line of a Coherent Innova 200 Ar^+ laser was used for excitation and for pumping a dye laser and a Ti-sapphire laser. A Coherent Innova 100 Kr^+ laser provided excitation at 752.5, 676.4, 647.1 and 568.2 nm. A Coherent 599 dye laser charged with DCM laser dye was used for excitation from 604 to 708 nm. A Spectra Physics Model 3900 CW Ti-sapphire laser was used for excitation between 720 to 750 nm. An Anaspec pre-monochromator was employed to remove plasma lines when exciting with the Ar^+ and Kr^+ laser lines. The laser power for all experiments was 20 mW when measured at the sample unless otherwise noted. The Raman

scattering was collected by a Nikkor-S lens and focused onto the entrance slit of a 1877 Spex Triplemate monochromator equipped with a 1200 groove/mm grating. A Princeton Applied Research CCD (model LN/CCD-1152) cooled to -120 °C was used for Raman signal detection. Signal integration periods were typically 200 s unless otherwise noted. A Gateway 2000 486DX2/50 computer with CSMA software (version 2.3a) was used for data collection. The Raman spectra were processed using CSMA and SpectraCalc software (version 2.21).

Temperature Dependence Conditions. To obtain temperature dependence data, a heating/cooling system was constructed to control the electrode surface temperature. A Furon Teflon diaphragm pump was used to circulate the heating/cooling fluids through a Pyrex flow cell containing the electrodes. Teflon tubing connected all components of the heating/cooling system. A glass jacketed Type J thermocouple submerged in bath oil and placed immediately following the flow cell was used to monitor the fluid temperature. For the heating experiments, 18 MΩ cm water was heated in a round bottom flask using a heating mantle. A stirring rod with fins circulated the water in the flask to improve temperature stability. The useful temperature range for electrode heating was approximately 20 to 85 °C. For the cooling experiments, an ethanol/liquid nitrogen slurry was formed in a dewar, and stirred occasionally to circulate the slurry. The slurry temperature was varied by careful addition of liquid nitrogen to the dewar. The effective temperature range for cooling the electrode was approximately 0 to -30 °C. A stream of N_2 gas was directed at the flow cell during cooling experiments to avoid atmospheric water condensation on the flow cell window. Cell flow rates varied according to the viscosity of the heating/cooling fluids.

Sample Purity Determination. The purity of the synthesized mercaptoalcohols was ascertained using a Hewlett-Packard (HP) GC/MS system. Separations were accomplished on a 5890 Series II Plus GC using a HP-5MS GC column (30 m length, 0.25 mm ID, 0.25 μm film thickness) and He as carrier gas. A 5972 Series MSD was used to generate mass spectra. Data analysis was carried out on a HP Vectra 486/66XM computer using G1034B HP Chemstation software.

The ^{1}H NMR data were collected using a Bruker V22520 NMR spectrometer operated at 300 MHz with a Varian VXR-300 controller for data collection. Experiments were conducted in either $CDCl_3$ or CD_3OD solvents, used as received from Aldrich Chemical. No tetramethylsilane (TMS) was used for NMR calibration. The center band of a quintet located at 3.30 ppm was used for spectra calibration for samples in CD_3OD while a singlet band at 7.25 ppm was used to calibrate spectra for samples in $CDCl_3$. The number of sample scans was varied according to individual sample concentrations. The NMR data were analyzed using Varian NMR software.

Electrochemical Conditions. Cyclic voltammetry (CV) and potential dependent SERS measurements of the alkanethiol monolayers were carried out in a three electrode H cell containing a Au wire auxiliary electrode and a Ag/AgCl/1.0 M NaCl reference electrode in one half of the cell and the working alkanethiol/Au electrode in the other half. The electrolyte solution, 0.5 M KOH (aq), was bubbled with nitrogen for approximately 30 minutes before use to remove dissolved oxygen. A blanket of nitrogen gas was kept over the electrochemical cell during potential scans. Reagent grade KOH from Fisher Scientific Co. was used as received for the electrolyte solutions. A BAS CV-1 potentiostat was used for potential

control and a HP 1068A X-Y plotter was used for current measurement. A potential sweep rate of 50 mV/s was typically used.

RESULTS AND DISCUSSION

Initial efforts to understand and utilize alkanethiol monolayers on polycrystalline metal surfaces began with a study of 1-octadecanethiol monolayers on roughened Ag. When excited by 514.5 nm light, strong SERS signals were observed, the most intense of which include the ν(C-S), ν(C-C), and r(CH_3) bands, as seen in Figure 1a. The observed results are in good agreement with literature reports.[18,19] The strong ν(C-S) band at 710 cm^{-1} is an indicator of the chain trans (T) mode, $\nu(C\text{-}S)_T$, while the much smaller band at 640 cm^{-1} is an indicator of the chain gauche (G) mode, $\nu(C\text{-}S)_G$. The strong $\nu(C\text{-}S)_T$ reveals that a relatively well ordered monolayer exists on the metal surface. The much smaller $\nu(C\text{-}S)_G$ band also suggests a relatively well ordered monolayer since the gauche conformation does not pack as well as the trans configuration. When the 1-octadecanethiol monolayers on roughened Ag are excited with 647.1 nm light, an unusual spectrum is observed. In the ν(C-S) region, two new bands appear and the $\nu(C\text{-}S)_T$ band shifts slightly to the red. The ν(C-C) and the r(CH_3) bands appear as before, as shown in figure 1b. The new bands in the ν(C-S) region are at 680 and 747 cm^{-1} and are sharp relative to other bands in the ν(C-S) region. The FWHM of the new bands are approximately 6 cm^{-1} whereas the FWHM of the ν(C-S) bands is approximately 30 cm^{-1}. In an effort to discover the source of the new bands, several 1-octadecanethiol monolayers were prepared on roughened Au electrodes.

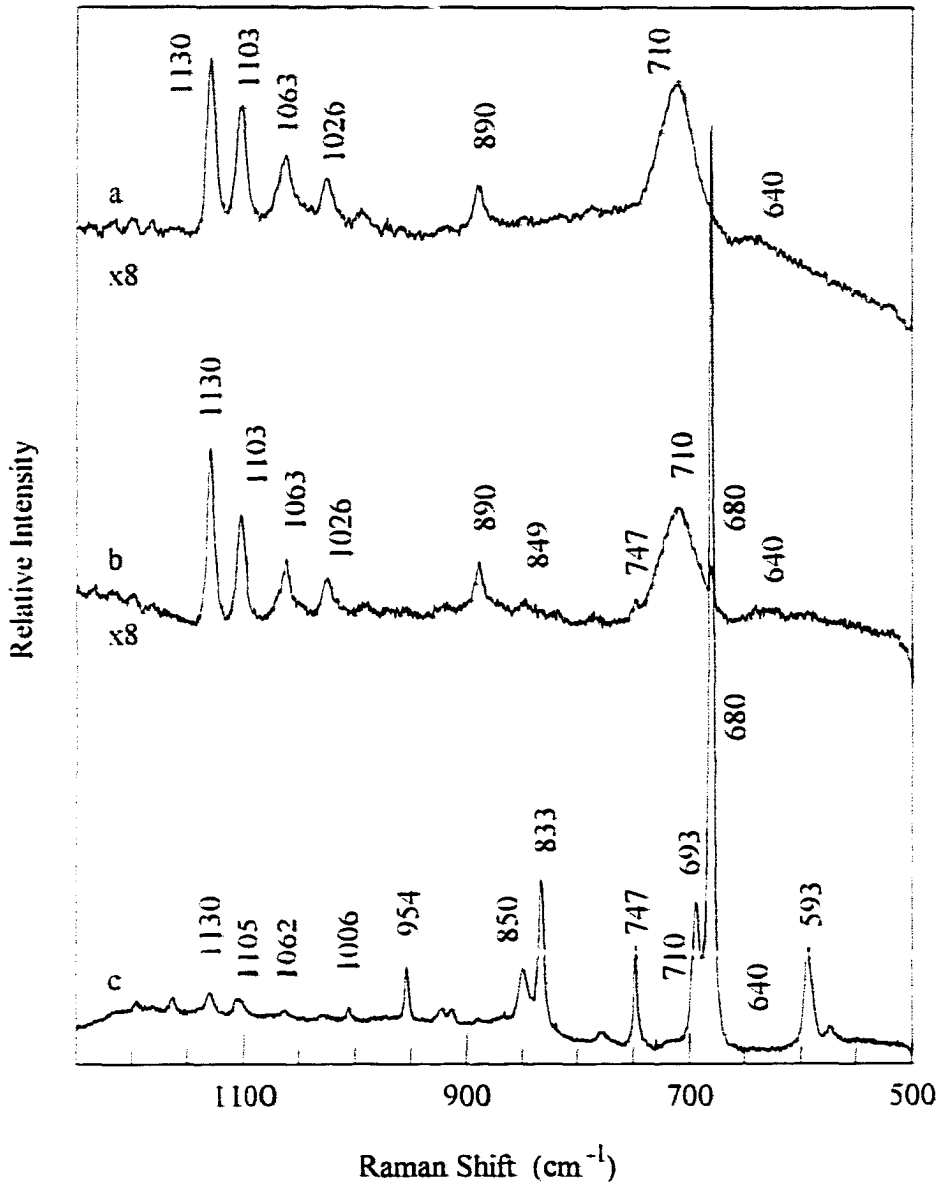

Figure 1. SERS spectra of CH_3-$(CH_2)_{17}$-SH monolayers on Ag and Au electrodes. a) Ag electrode with 514.5 nm excitation, b) Ag electrode with 647.1 nm excitation, c) Au electrode with 647.1 nm excitation. Spectra a & b are x8 for clarity.

Figure 1c shows a spectrum of an 1-octadecanethiol monolayer on roughened Au with 647.1 nm excitation. The dominant feature is the very strong band at 680 cm^{-1}. In addition to the above bands, other bands at 692, 746, 833, 850 and 954 cm^{-1} are present on Au which are not seen on Ag with 514.5 nm excitation. The $\nu(C\text{-}S)_T$ and $\nu(C\text{-}S)_G$ bands, expected about 710 and 640 cm^{-1} respectively, are overshadowed by the much stronger 680 and 693 cm^{-1} bands. The Raman bands in the $\nu(C\text{-}C)$ region and the $r(CH_3)$ band appear as before, but are also much weaker than the 680 cm^{-1} band. A review of the literature did not indicate a possible source of the strong novel bands, which appear not to have been reported prior to now. In the previous SERS work involving SAMs of long-chain alkanethiols on Au and Ag surfaces, laser excitation at 514.5, 600 and 720 nm did not reveal the novel bands.[18,19] These excitation wavelengths are just outside the excitation profile in which the new bands appear, as will be shown later.

Surface Impurity Experiments. It was considered that a possible and highly undesirable source of the new bands may be impurities in the monolayer preparation solutions. A common impurity found in alkanethiols is the dialkane disulfide (RSSR), the result of thiol oxidation. Dioctadecyl disulfide was prepared according to literature methods, purified, and exposed to roughened Au electrodes.[23] Figure 2a shows the SERS spectrum of dioctadecyl disulfide monolayers on roughened Au with 647.1 nm excitation. The new bands in the $\nu(C\text{-}S)$ region are also present in the dioctadecyl disulfide spectrum. The band at 679 cm^{-1} is very strong compared to all other bands while bands at 693, 748 and 833 cm^{-1} are still present. It has been shown for dialkyl disulfides that the S-S bond is cleaved as the disulfide forms a monolayer on Au.[24] Thus, the dioctadecyl disulfide should form monolayers on Au similar to

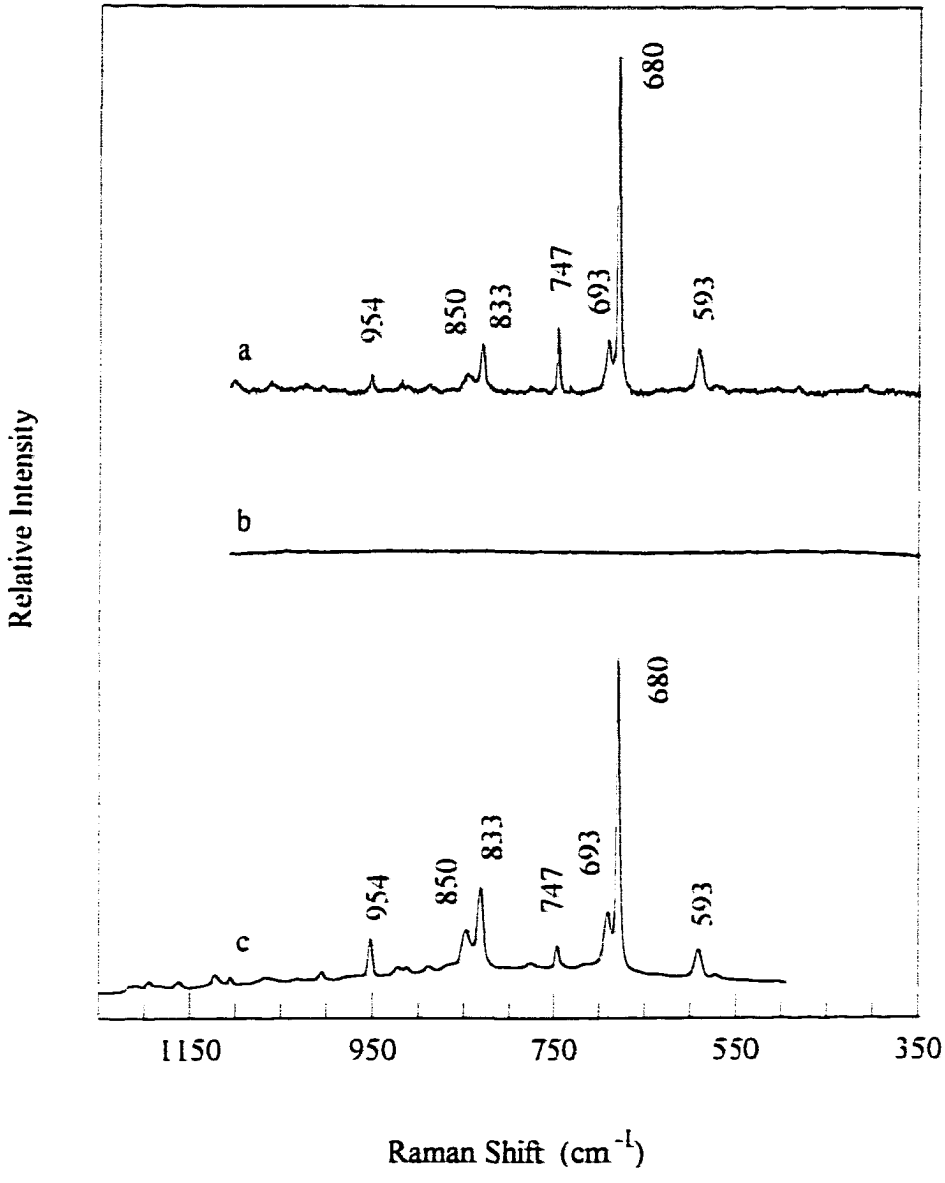

Figure 2. SERS spectra to determine possible impurities on Au electrodes. λ_{ex} = 647.1 nm at 20 mW power. a) $(CH_3\text{-}(CH_2)_{17}\text{-}S)_2$ SAM; b) bare Au electrode (no alkanethiol exposure); c) $CH_3\text{-}(CH_2)_9\text{-}SH$ SAM after exposure to Br^- solution (to remove Cl^- from Au surface).

the corresponding 1-alkanethiol and produce a similar SERS spectrum. These results suggest three possible sources of the new bands: a) impurities on the Au and Ag surfaces from electrode pretreatment, b) impurities in the 1-alkanethiols, which survived the dialkyl disulfide formation procedure and subsequent disulfide purification procedures, or c) the 1-alkanethiol monolayers are the source of the new bands.

Figure 2b shows the spectra of a clean roughened Au electrode, in the absence of an alkanethiol monolayer. This electrode was subject to the exact same polishing, cleaning and roughening treatments as the other Au electrodes that were subsequently exposed to thiol solutions. The bare Au electrode was also exposed to HPLC grade methanol, the thiol deposition solution solvent, for the same amount of time as the Au electrodes with the alkanethiol monolayers. The results of this experiment indicate that there are no substantial impurities in the methanol used for monolayer deposition. The roughening procedure for Au electrodes, performed in aqueous 0.1 M KCl, may leave substantial amounts of Cl^- on the electrode surface. To reduce the possible interference of Cl^- on the Au surface, the Au foil electrodes were roughened by the usual procedure, then placed in an aqueous 0.1 M KBr solution for approximately 25 hours. The Br^- should displace the Cl^- on the Au surface, reducing the possible interaction of Cl^- with the Au surface. After the normal roughening procedure and Br^- exposure the Au electrodes were rinsed with water and methanol, then exposed to the 1 mM 1-decanethiol deposition solution. The resulting SERS spectrum is shown in Figure 2c. No change in the new bands is noted in the spectrum after Br^- exposure. Thus, the possible interaction of Cl^- with the alkanethiol monolayer as the source of the new SERS bands is ruled out. These experiments indicate that the source the new bands is not due

to Au surface impurities. Similar exposure experiments with Ag electrodes indicated no impurities from the deposition solvent or the electrode roughening procedures (results not shown).

Alkanethiol Impurity Experiments. Several experiments were then conducted to detect possible impurities in the 1-alkanethiols and their deposition solutions which may give rise to the novel SERS bands. An initial series of GC/MS analyses were conducted to detect impurities in the deposition solutions. Alkanethiol deposition solutions of 1 mM concentration in methanol were analyzed before and after exposure to Au electrodes. The GC/MS chromatograms of all the alkanethiol deposition solutions reveal very minor amounts of impurities consisting of long-chain 1-alcohols, 1-hydrocarbons, and 1-bromoalkanes with similar carbon number to the alkanethiols used for deposition. The 1-alcohols and 1-hydrocarbons are not expected to be the source of the new SERS bands since they are weakly adsorbed to the Au surface and are easily displaced from the electrode surface by alkanethiol monolayer formation. The 1-bromoalkanes are most likely unreacted starting material from 1-alkanethiol synthesis and are also expected to be weakly adsorbed on Au. Thus, these 1-bromoalkanes should be readily displaced from the Au electrode surface. Figure 3 compares the SERS spectra of a 1-bromododecane monolayer on roughened Au to a 1-dodecanethiol monolayer on Au and as can be seen, the absence of the strong 680 cm^{-1} band is the most notable difference. The other novel SERS bands at 593, 747, 833 and 954 cm^{-1} are also absent from the 1-bromododecane spectrum. Thus, the GC/MS results combined with the 1-bromoalkane on Au SERS spectrum indicate that these minor straight chain impurities are not the source of the new SERS bands.

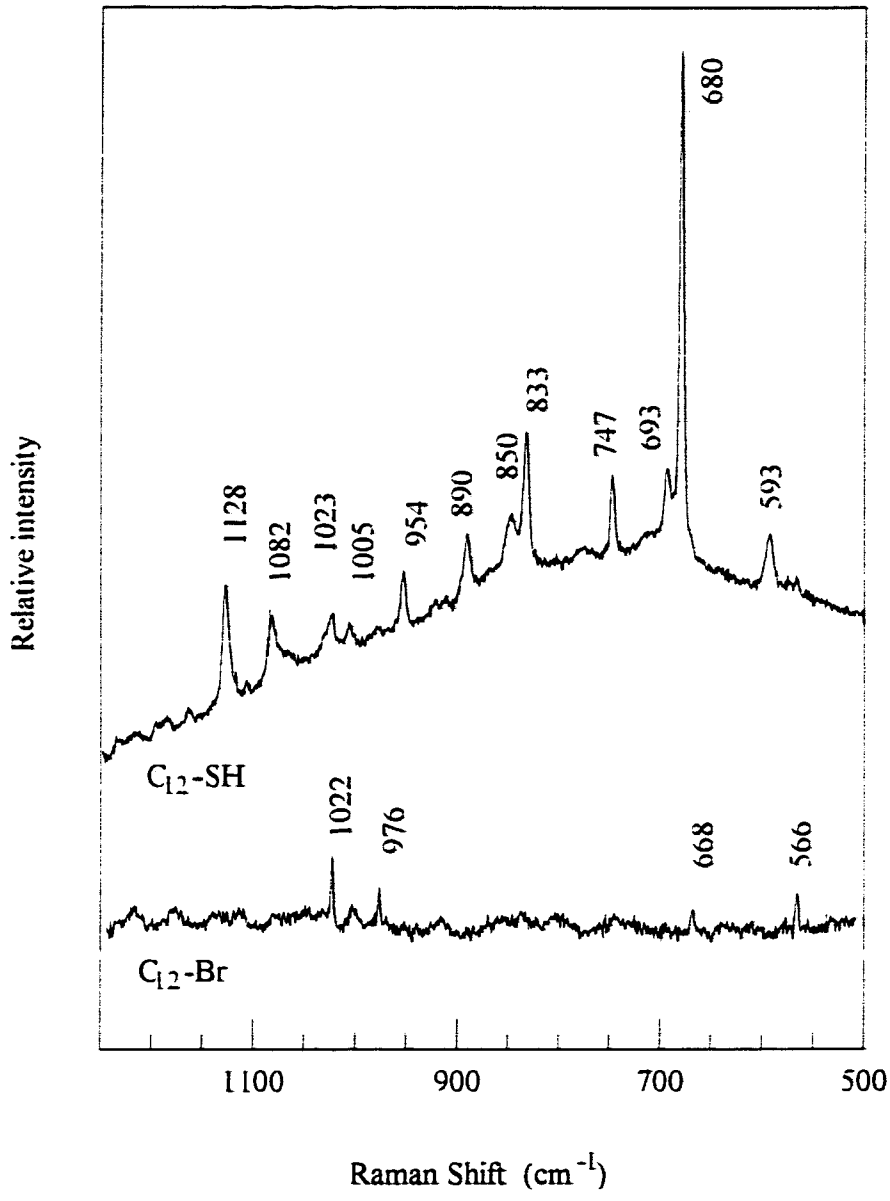

Figure 3. Comparison of SAMs of $CH_3(CH_2)_{11}$-Br and $CH_3(CH_2)_{11}$-SH on roughened Au electrodes. $\lambda_{ex} = 647.1$ nm at 20 mW.

Different alkanethiols from different sources were used to form monolayers on roughened Au electrodes. It is believed that alkanethiols from different sources would have different impurities. 1-Decanethiol and 1-dodecanethiol, from Aldrich Chemical Co., formed monolayers on roughened Au which display the same characteristic strong, sharp SERS bands at 680, 747, 954 cm^{-1} as the 1-octadecanethiol monolayers on Au when excited at 647.1 nm. 11-Mercapto-1-undecanol and 12-mercapto-1-dodecanol, compounds synthesized and purified in our lab, also yielded the same strong new SERS bands at their characteristic frequencies. Alkanethiol monolayers formed from 1-decanethiol and 11-mercapto-1-undecanol on Au colloids also produce the strong SERS bands seen in the 1-octadecanethiol spectra. Figure 4 illustrates the similarities between the different alkanethiol monolayers formed on Au surfaces, notably the SERS bands are seen at approximately 593, 679, 747, 833 and 954 cm^{-1}. There are differences which can be seen in the monolayer spectra, occurring in the ν(C-C) region between 1000-1130 cm^{-1} which are due to the different carbon chain lengths.[25] The novel Raman bands are also notably weaker in the $n = 8$ spectrum. These simple experiments show that the source of the novel bands is present in all the long-chain alkanethiol monolayers tested to date.

The next step in the effort to detect possible impurities in the monolayers utilized ^1H NMR to study the thiol deposition solutions and Ag colloids with thiol monolayers. ^1H NMR was chosen because many sample scans could be run to improve sensitivity and aromatic rings can readily be observed. Aromatic compounds, which yield SERS bands in the 600-700 cm^{-1} region, can thus be ruled out as monolayer impurities if such are not detected by ^1H NMR. In Figure 5a, the ^1H NMR spectrum of 1.0 M 1-decanethiol in $CDCl_3$ reveals a very small single

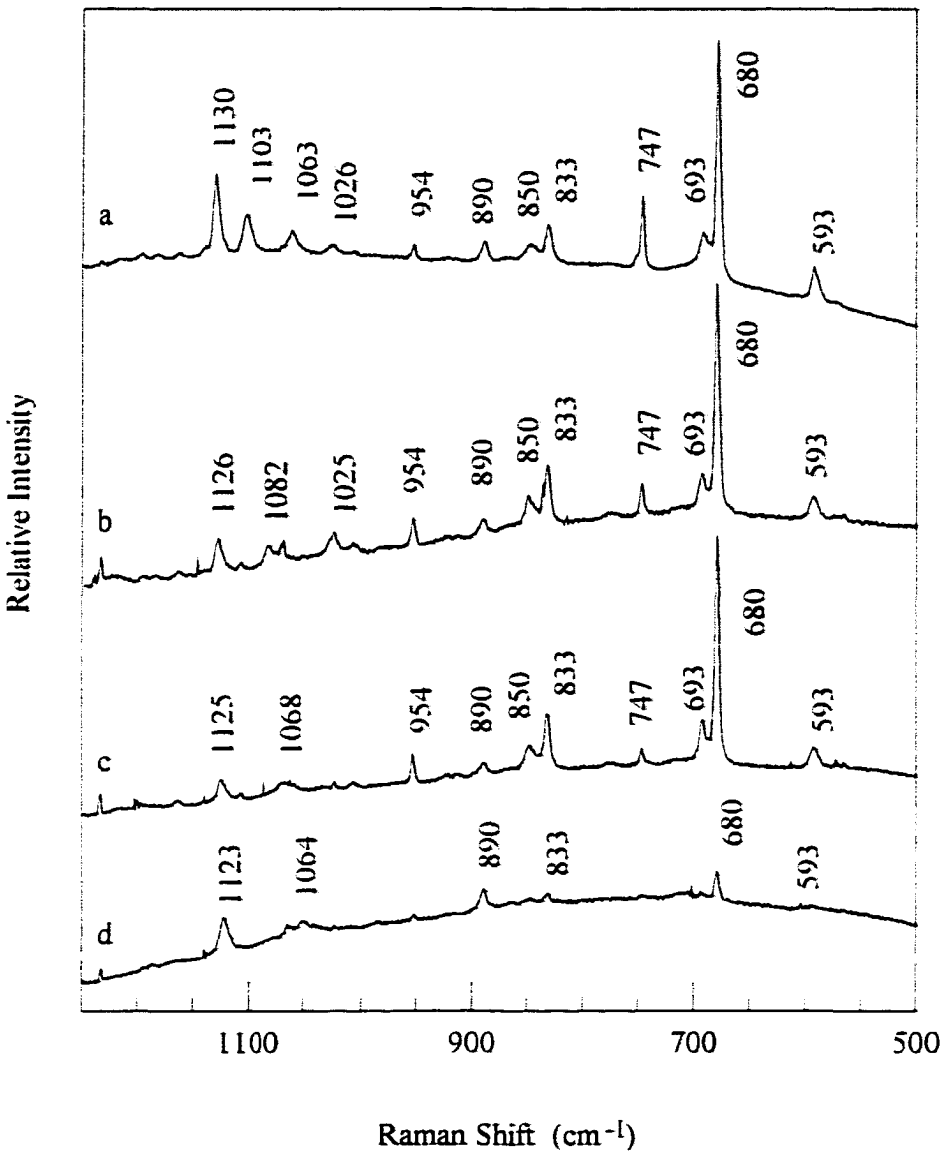

Figure 4. SERS of different long-chain $CH_3(CH_2)_n$-SH monolayers on Au. λ_{ex} = 647.1 nm at 20 mW. a) $n = 17$; b) $n = 11$; c) $n = 9$ and d) $n = 8$.

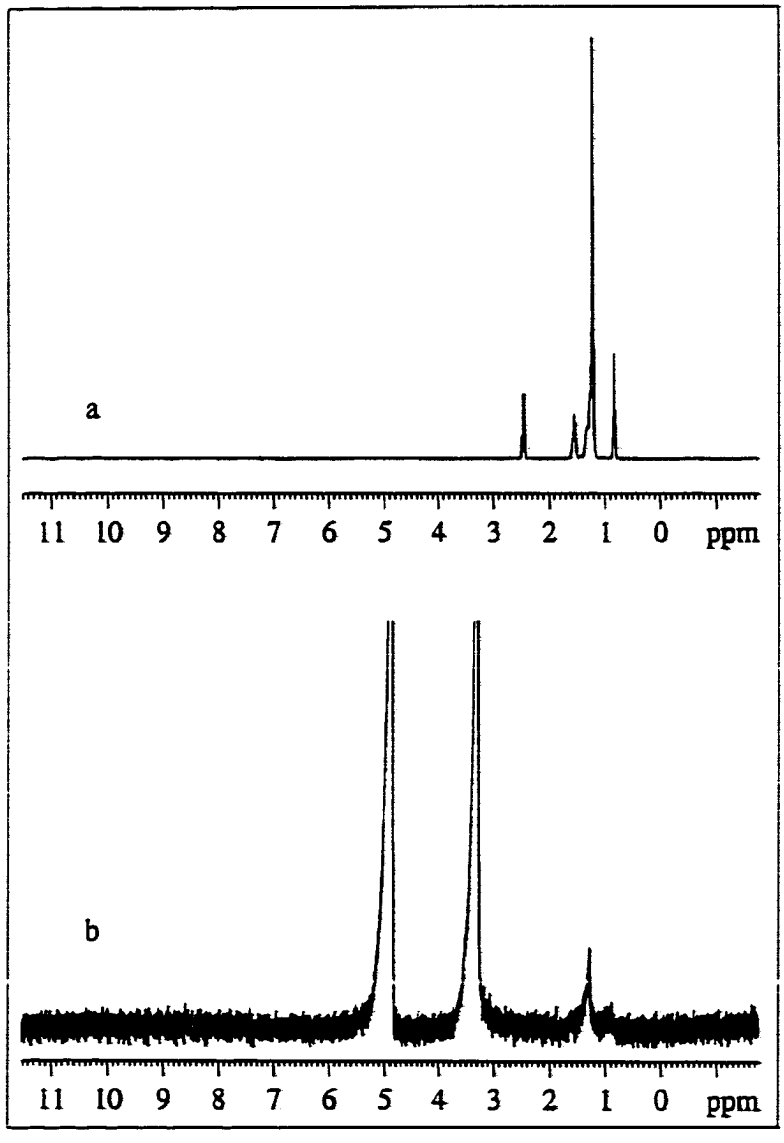

Figure 5. ^{1}H NMR of alkanethiols. a) 1.0 M 1-decanethiol solution in $CDCl_3$. b) 12-mercapto-1-dodecanol monolayer on Ag colloid in CD_3OD. The Ag colloid spectra is expanded to show the alkanethiol bands. The bands at ca. 3.3 and 5 are due to ^{1}H in the CD_3OD solvent.

peak in the region near 7 ppm. The higher decanethiol concentration, 100 times greater that used for monolayer deposition, was used in this experiment to increase sensitivity. The single NMR band at 7.25 ppm is assigned to residual $CHCl_3$ in the deuterated solvent. No other NMR bands are seen in this region of the spectra. Thus, ^1H NMR does not reveal any possible contaminating aromatic compounds in the monolayer deposition materials. The second set of ^1H NMR experiments involved alkanethiol monolayers on metal colloids. Ag colloid was used in the NMR experiments because of their greater ability to remain in solution in organic solvents. Au colloid tended to aggregate and precipitate out of solution in both CD_3OD and $CDCl_3$. 12-Mercapto-1-dodecanol was chosen for this NMR colloid monolayer study since a) there are many protons to detect and b) there is an -OH group at the end of the alkyl straight chain to help stabilize the colloid in the CD_3OD solvent. The modified Ag colloid tended to aggregate more and precipitate in CD_3OD when a methyl terminated alkanethiol was used for monolayer formation. No NMR bands were seen on the thiol modified Ag colloid in the 7 ppm region, as seen in figure 5b, indicating no aromatic impurities in the alkanethiol monolayers. These NMR experiments indicate that the source of the new resonance bands is not due to impurities in the 1-alkanethiols used for monolayer deposition.

1-Alkanethiol Monolayer Experiments. Another series of experiments was then designed to investigate changes in the SERS spectra on Au due to changes in 1-alkanethiol carbon chain length. As demonstrated in previous figures, 1-alkanethiol monolayers on Au with carbon chain length from 10 to 18 C atoms yielded the strong novel SERS bands. Monolayers of 1-nonanethiol, 1-octanethiol and 1-butanethiol were then formed on roughened

Au electrodes and the SERS spectra of these monol[illegible]
the newly observed SERS bands, but at lower intensit[illegible]
and 1-butanethiol on Au do not yield any of the ne[illegible]
spectra of 1-nonanethiol, 1-octanethiol and 1-butaneth[illegible]
experiments indicate that a chain length minimum [illegible]
to observe the new SERS bands of the 1-alkanethiols [illegible]
previous reports of 1-alkanethiol monolayer formation [illegible]
packing occurs when the carbon chain length is about [illegible]
chains of less than nine carbon atoms form SAMs th[illegible]
highly crystalline, while chains of nine or more carbon [illegible]
crystalline monolayers which are organized into [illegible]
It is believed that the structural differences arise from [illegible]
between the long alkanethiol chains which result in more [illegible]
films.

To further investigate the role of monolayer in [illegible]
on Au, several mixed monolayer experiments were con[illegible]
were exposed to deposition solutions of 1:1 1-decaneth[illegible]
decanethiol / 1-butanethiol in which the total 1-alkaneth[illegible]
1 mM, as in previous deposition solutions. The results [illegible]
Figure 7. A monolayer consisting of only CH_3-CH_2- [illegible]
comparison with the 1:1 CH_3-$(CH_2)_9$-SH CH_3-CH_2- [illegible]
CH_3-$(CH_2)_9$-SH / CH_3-$(CH_2)_3$-SH mix in spectrum [illegible]